Electrochemical and Spectroelectrochemical Properties of the Titanium Sandwich Complexes (Cp)Ti(L) and (Cp*)Ti(L), Where L Is either Cyclooctatetraene (C_8H_8) or the Tropylium Ion ($C_7H_7^+$)

J. E. Anderson,* E. T. Maher, and L. B. Kool

Department of Chemistry, Boston College, Chestnut Hill, Massachusetts 02167

Received July 19, 1990

Electrochemical and spectroelectrochemical data for (Cp)Ti(L) and (Cp*)Ti(L), where Cp is the anion of cyclopentadienyl and Cp* is the anion of pentamethylcyclopentadienyl and L is either cyclooctatetraene (C_8H_8) or the tropylium ion ($C_7H_7^+$) are presented in this paper. The electrochemical properties of complexes 1–4 [(Cp)Ti(L) L = C_8H_8 (1), C_7H_7 (2); (Cp*)Ti(L), L = C_8H_8 (3), C_7H_7 (4)] are shown to be dependent upon the electron-donating ability of L and the solvent–supporting electrolyte system. Complexes 2 and 4 can be reduced and oxidized by one electron, while complexes 1 and 3 only exhibit a one-electron oxidation. The presence of perchlorate anion, from the supporting electrolyte, strongly affects the electrochemical response for complexes 1 and 3 but not complexes 2 and 4. The synthesis of (Cp*)Ti(C_8H_8)(ClO_4) is described, and this species is characterized by ^{1}H NMR, infrared, and electronic spectra and by electrochemical methods. An electron-transfer mechanism for complexes 1–4 is presented, and the use of spectroelectrochemical methods to examine the site of electron transfer for this set of organometallic species is discussed.

The results from an electrochemical and spectroelectrochemical investigation of (Cp)Ti(L) and (Cp*)Ti(L), where Cp is the anion of cyclopentadienyl and Cp* is the anion of pentamethylcyclopentadienyl and L is either cyclooctatetraene (C_8H_8) or the tropylium ion ($C_7H_7^+$), are presented and the fundamental electrochemical properties of the compounds are discussed. In addition to the synthesis, structure, and reactivity of (Cp)Ti(L) and (Cp*)-Ti(L),[1-3] molecular orbital calculations have been performed for the cyclopentadienyl species[4-6] and the results are in close agreement with ESR,[7] ENDOR,[8-10] and photoelectron studies.[11,12] The agreement among these different methods makes possible a detailed understanding of the electronic structure of these complexes. This insight will be important in our analysis of the spectroelectrochemical results.

Our data will demonstrate that, although complexes 1–4 are structurally very similar, the cyclooctatetraene adducts have electrochemical and spectroelectrochemical properties significantly different from those of the tropylium ion adducts. These differences are consistent with the electron-donating ability of L as well as the formal charge on the Ti.[13,14] A change from Cp to Cp* does not cause a significant change in the electron-transfer properties, other than the expected shift in the energy of electron transfer.[15]

In contrast to ferrocene[15-17] and other sandwich species,[18-22] few electrochemical data are available for complexes 1–4. For (Cp)Ti(C_7H_7), a reversible one-electron reduction is reported to occur at −2.00 V vs Ag/AgCl in THF/TBA(PF_6) at a reduced temperature and at room temperature chemical reactions follow this reduction.[10] For both (Cp)Ti(C_8H_8) and (CH_3-C_5H_4)Ti(C_8H_8), a reversible one-electron-oxidation process is reported to occur at −0.50 and −0.56 V vs SCE, respectively, in THF/TBA(PF_6).[23] Our results are in general agreement with these data, but some differences due to the choice of the solvent and supporting electrolyte are observed. Hence, the electrochemical properties of (Cp)Ti(L) and (Cp*)Ti(L) in different solvents and as a function of supporting electrolyte will be presented and an electron-transfer mechanism will be discussed.

Experimental Section

Titanium Complexes. (Cp)Ti(L) and (Cp*)Ti(L) were synthesized and characterized by published methods.[2,3]

Materials. The acetonitrile (CH_3CN), dichloromethane (CH_2Cl_2), and tetrahydrofuran (THF) used for electroanalysis were purchased (Aldrich) as spectroscopic grade, purified and dried by standard methods,[24,25] stored over calcium hydride (CH_3CN),

(1) Bottril, M.; Gavens, P. D.; McMeeking, J. Titanium: In *Comprehensive Organometallic Chemistry*; Wilkinson, G., Ed.; Pergamon Press: New York, 1982; Vol. 3, p 281.
(2) Elschenbroich, C.; Salzer, A. *Organometallics, A Concise Introduction*; VCH Publishers: New York, 1989; pp 358–369.
(3) Kool, L. B.; Rausch, M. D.; Rogers, R. D. *J. Organomet. Chem.* **1985**, *297*, 289.
(4) Clack, D. W.; Warren, K. D. *Inorg. Chim. Acta* **1977**, *24*, 35.
(5) Clack, D. W.; Warren, K. D. *Theor. Chim. Acta* **1977**, *46*, 313.
(6) Zeinstra, J. D.; Nieupoort, W. C. *Inorg. Chim. Acta* **1978**, *30*, 103.
(7) Samuel, E.; Labauze, G.; Vivien, D. *J. Chem. Soc., Dalton Trans.* **1979**, 956.
(8) Labauze, G.; Raynor, J. B.; Samuel, E. *J. Chem. Soc., Dalton Trans.* **1980**, 2425.
(9) Gourier, D.; Samuel, E. *J. Am. Chem. Soc.* **1987**, *109*, 4571.
(10) Gourier, D.; Samuel, E. *Inorg. Chem.* **1988**, *27*, 3018.
(11) Evans, S.; Green, J. C.; Jackson, S. E. *J. Chem. Soc., Dalton Trans.* **1974**, 304.
(12) Andrea, R. R.; Terpstra, A.; Oskam, A.; Bruin, P.; Teuben, J. H. *J. Organomet. Chem.* **1986**, *307*, 307.
(13) Connely, N. G.; Geiger, W. E. *Adv. Organomet. Chem.* **1984**, *23*, 1.
(14) Anderson, J. E.; Gregory, T. P.; McAndrews, C. M.; Kool, L. B. *Organometallics* **1990**, *9*, 1702.
(15) A. J. Deeming, Ferricinium and Protonated Ferrocene Ions. In *Comprehensive Organometallic Chemistry*; Wilkinson, G., Ed., Pergamon Press: New York, 1982; Vol. 4, pp 480–481.
(16) Sabbatini, M. M.; Cesarotti, E. *Inorg. Chim. Acta* **1977**, *24*, L9.
(17) Grimes, H.; Loagan, S. R. *Inorg. Chim. Acta* **1980**, *45*, L223.
(18) Bowyer, W. J.; Geiger, W. E. *J. Am. Chem. Soc.* **1985**, *107*, 5657.
(19) Geiger, W. E.; Rieger, P. H.; Tulathan, B.; Rausch, M. D. *J. Am. Chem. Soc.* **1984**, *106*, 7000.
(20) Merkert, J.; Nielson, R. M.; Weaver, M. J.; Geiger, W. E. *J. Am. Chem. Soc.* **1989**, *111*, 7084.
(21) Pierce, D. T.; Geiger, W. E. *J. Am. Chem. Soc.* **1989**, *111*, 7636.
(22) Miller, G. A.; Therien, M. J.; Trogler, W. C. *J. Organomet. Chem.* **1990**, *383*, 271.
(23) Samuel, E.; Guery, D.; Vedel, J. *J. Organomet. Chem.* **1984**, *263*, C43.
(24) Riddick, J. A.; Bunger, W. B.; Sakano, T. K. *Organic Solvents*, 4th ed.; Wiley-Interscience: New York, 1986.

0276-7333/91/2310-1248$02.50/0

phosphorus pentoxide (CH_2Cl_2), or sodium/benzophenone (THF) under an inert atmosphere, and distilled immediately prior to use. Tetrabutylammonium perchlorate (TBAP) was purchased from Fluka, and tetrabutylammonium tetrafluoroborate [TBA(BF_4)] was purchased from Aldrich. Both salts were doubly recrystallized from ethanol and were dried in a vacuum oven at 50 °C.

Equipment and Techniques. Electrochemical experiments were performed with either a BAS-100A or a EG&G Princeton Applied Research 273 potentiostat/galvanostat coupled to an EG&G Princeton Applied Research Model RE0091-XY recorder and an IBM PS/2 Model 50 computer. A platinum-button working electrode (approximate area 0.008 cm^2) a platinum-wire counter electrode, and an SCE reference electrode separated from the solution with a bridge comprised the three-electrode system. All potentials are reported vs the SCE electrode and have a precision of 0.005 V. The ferrocene/ferrocenium couple was also used as an internal standard. The concentration of supporting electrolyte was 0.2 M unless otherwise stated. Bulk electrolysis experiments were carried out in a two-compartment cell with a large platinum working electrode (0.4 cm^2), a platinum counter electrode and an SCE reference electrode separated from the solution with a bridge.

Spectroelectrochemical data were recorded with a Perkin-Elmer Lambda 3B UV–vis spectrometer using an BAS CV-27 potentiostat or an IBM EC/225 voltammetric analyzer coupled to an IBM 7427 MT X-Y-T recorder. The electrodes were a large platinum-minigrid working electrode (0.2 cm^2), a platinum-wire counter electrode, and either an Ag/AgCl reference electrode separated from the solution with a bridge or a Pt-wire pseudo reference electrode. The supporting electrolyte concentration was 0.2 M unless otherwise stated. UV–vis spectra of (Cp)Ti(L) and (Cp*)Ti(L) were also recorded in standard cells designed for inert atmosphere in the presence and absence of supporting electrolyte. No significant differences in the electronic spectra were found due to the presence of the supporting electrolyte.

The electrochemical cells were all home-built and were designed for analysis of air-sensitive species.[26] All solid and solution transfers were carried out by standard Schlenk methodologies.[27] UV–vis measurements were performed with the Perkin-Elmer Lambda 3B spectrometer. Infrared spectra were obtained on a Nicolet 510 FT-IR spectrometer, and NMR data were collected on a Varian XL 300-MHz NMR spectrometer.

Abbreviations used in this text follow standard electrochemical convention.[28] For example, E_p is the peak potential, υ is the scan rate, and i_p is the peak current.

Results

Reduction of (Cp)Ti(C_7H_7) and (Cp*)Ti(C_7H_7). Figure 1A is the cyclic voltammetric response obtained for a solution of (Cp)Ti(C_7H_7) in THF/TBAP, when the potential is scanned in a negative direction. One reduction wave (wave 1, Figure 1A) is observed at $E_{pc} = -1.97$ V vs SCE at a scan rate of 100 mV/s. Wave 1 is a diffusion-controlled process, evidenced by a constant value of the peak current in relation to the square root of the scan rate ($i_p/\upsilon^{1/2}$). The value of $E_p - E_{p/2}$ is 89 mV,[28,29] and E_{pc} for wave 1 is observed to shift to negative potentials as the scan rate is increased. It has been previously shown[10] that wave 1 corresponds to a one-electron transfer. Our data are fully consistent with this and indicate an electrochemical EC process for the reduction of (Cp)Ti(C_7H_7).[30]

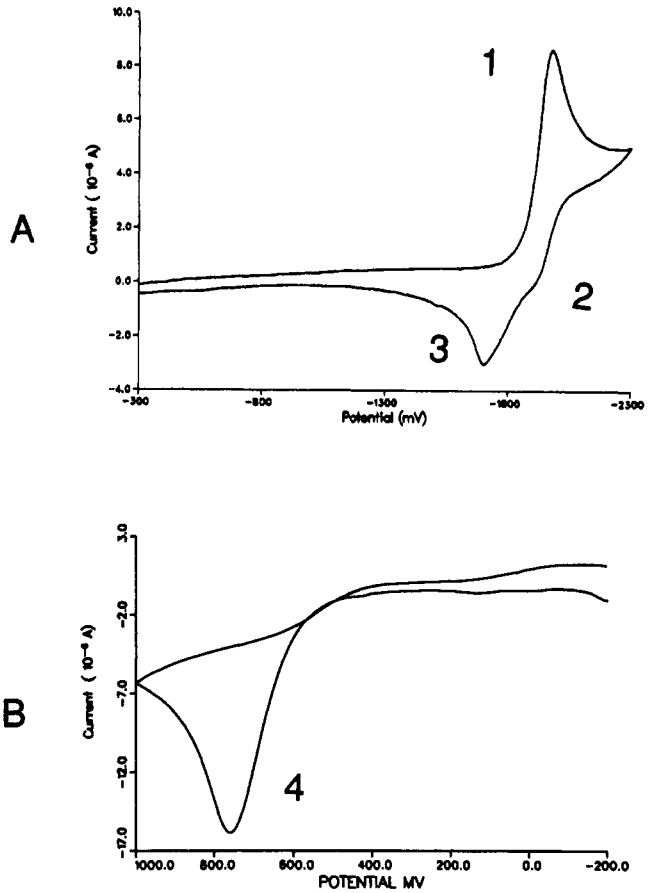

Figure 1. Cyclic voltammograms of a solution of (Cp)Ti(C_7H_7) in THF/0.34 M TBAP (scan rate 100 mV/s): (A) scan from −0.30 to −2.30 V; (B) scan from −0.20 to +1.00 V.

Two oxidative processes are observed (waves 2 and 3, Figure 1A) after scanning negative of wave 1. The ratio of the current for wave 2 (i_{p_2}) to that of wave 3 (i_{p_3}) is scan-rate-dependent. Hence, as the scan rate is increased, i_{p_2}/i_{p_3} also increases. Since waves 2 and 3 represent re-oxidation of species generated by reduction of (Cp)Ti(C_7H_7), the scan rate dependence of i_{p_2}/i_{p_3} implies that wave 2 is due to an intermediate species while wave 3 is due to a chemical reaction product. Multiple scans show only waves 1–3, and hence, waves 2 and 3 result in regeneration of (Cp)Ti(C_7H_7). Wave 2 is located at $E_{pa} = -1.90$ V vs SCE and is assigned to the oxidation of [(Cp)Ti(C_7H_7)]$^-$ (i.e., waves 1 and 2 are a reversible couple). Wave 3 is a diffusion-controlled, one-electron process characterized by a value of $E_{pa} = -1.70$ V vs SCE at a scan rate of 100 mV/s, a constant value of $i_p/\upsilon^{1/2}$, and a value of $E_p - E_{p/2}$ of 77 mV. The location of wave 3 is 270 mV positive of wave 1 and is assigned to the reoxidation of the product of the chemical reaction following reduction of (Cp)Ti(C_7H_7).

Consistent with our data and the assignment of wave 2 (Figure 1A) as the re-oxidation of the monoanion, the reversible one-electron reduction of (Cp)Ti(C_7H_7) at −2.00 V vs a Ag/AgCl reference in THF/TBA(PF_6) at −20 °C has been reported.[10] At room temperature, a chemical reaction was reported to follow the reduction, but no characterization of the product was reported.

(Cp*)Ti(C_7H_7) in THF/TBAP has a one-electron-reduction wave at $E_{pc} = -2.25$ V vs SCE at 100 mV/s that corresponds to wave 1 in Figure 1A. Wave 2 is not observed, but wave 3 is found and occurs at $E_{pa} = -2.03$ V. Multiple scans in the cyclic voltammogram indicate only the presence of waves 1 and 3 for complex **4**. The cyclic

(25) Kadish, K. M.; Anderson, J. E. *Pure Appl. Chem.* **1987**, *59*, 5, 707.
(26) Anderson, J. E.; Gregory, T. P. *Inorg. Chem.* **1989**, *28*, 3905.
(27) Shriver, D.; Drezdzon, M. A. *The Manipulation of Air-Sensitive Compounds*, 2nd ed.; Wiley: New York, 1986.
(28) Bard, A. J.; Faulkner, L. R. *Electrochemical Methods, Fundamentals and Applications*; Wiley: New York, 1980.
(29) Values of $E_p - E_{p/2}$ and/or E_p are larger than predicted by theory due to the high resistance of the nonaqueous system. However, our values of $E_p - E_{p/2}$ and/or E_p are consistent with that observed for ferrocene added as an internal reference.
(30) E stands for electron transfer and C stands for a chemical reaction coupled to the electron transfer: Nicholson, R. S.; Shain, I. *Anal. Chem.* **1964**, *36*, 706.

Table I. Electrochemical Data for (Cp)Ti(L) and (Cp*)Ti(L)

complex	solvent	supporting electrolyte	E_p,[a] V 1	2	3	4	Fc[b]
(Cp)Ti(C_7H_7)	THF	TBAP	−1.97	−1.90	−1.70	0.76	0.77
	CH_3CN	TBAP	−2.12	c	−2.02	0.15	0.40
	CH_2Cl_2	TBAP	−2.13	c	c	0.50	0.46
	THF	TBA(BF_4)	−2.06	c	−1.80	0.43	0.64
(Cp*)Ti(C_7H_7)	THF	TBAP	−2.25	c	−2.03	0.35	0.53
	CH_3CN	TBAP	−2.25	c	−2.03	0.13	0.40
	CH_2Cl_2	TBAP	c	c	c	0.36	0.47

complex	solvent	supporting electrolyte	E_p,[a] V 5	6	7	Fc[b]
(Cp)Ti(C_8H_8)	THF	TBAP	−0.30	−0.17	−0.42	0.69
	CH_3CN	TBAP	−0.49	c	−0.64	−0.54
	CH_2Cl_2	TBAP[d]	−0.44	c	−0.52	0.63
	THF	TBA(BF_4)		−0.48[e]		0.57
(Cp*)Ti(C_8H_8)	THF	TBAP	−0.70[f]	−0.63[f]	−0.77[f]	0.55
	CH_3CN	TBAP	−0.54	−0.41	−0.57	0.46
	CH_2Cl_2	TBAP[d]	−0.61	c	−0.72	0.53
	THF	TBA(BF_4)		−0.68[e]		0.54

[a] Scan rate of 100 mV/s. [b] $E_{1/2}$ (V) for ferrocene. [c] Not observed under these conditions. [d] Compound is oxidized upon addition to the solvent; electrochemical data are for the oxidized species. [e] Waves 5 and 7 are not observed in the absence of perchlorate (see text). [f] Scan rate of 60 mV/s.

voltammetric data for the reduction of complexes **2** and **4** in CH_3CN with TBAP are the same as those observed in THF, except that wave 2 is not observed. Hence, the chemical reaction following electron transfer is faster in acetonitrile than in THF.

Only the reduction of complex **2** is observed in CH_2Cl_2, but in this case neither wave 2 nor wave 3 is observed. Reduction of complex **4** is not found due to the solvent discharge limit of CH_2Cl_2. These data imply reduction in CH_2Cl_2 is followed by a chemical reaction different from those in THF or CH_3CN. The electrochemical data for (Cp)Ti(C_7H_7) and (Cp*)Ti(C_7H_7) under the different solvent conditions are summarized in Table I.

Spectroelectrochemical data for the reduction of (Cp)Ti(C_7H_7) from 220 to 320 nm in THF/TBAP are shown in Figure 2. In this spectral region (Cp)Ti(C_7H_7) is characterized by bands at 242 and 315 nm, but in Figure 2 only the band at 242 nm is observed due to the small path length of the cell. Upon reduction at −2.20 V vs SCE, the band at 242 nm decreases in intensity and broadens. An increase in absorbance centered around 280 nm is found, and an isosbestic point at 255 nm is observed as shown in Figure 2A. Figure 2B shows the spectral changes that occur upon reoxidation at −0.20 V and indicates that (Cp)Ti(C_7H_7) is regenerated, in agreement with the multiple-scan cyclic voltammetric data. Some decomposition, however, is indicated in Figure 2B by the residual increase in absorbance near 280 nm after oxidation.

The reduction of (Cp)Ti(C_7H_7) at −2.20 V results in the generation of a strong band in the visible region centered at 510 nm, with a shoulder at 650 nm. The band at 510 nm is significantly stronger than the visible band of (Cp)Ti(C_7H_7) at 700 nm. The spectral changes correspond to a change from a light blue to a dark purple solution upon reduction. Reoxidation results in generation of the original visible spectrum with no indication of decomposition.

Electronic spectra have been reported[10] for (Cp)Ti(C_7H_7) and [(Cp)Ti(C_7H_7)]$^-$ that are significantly different from our data. The neutral complex was reported to have three absorption bands at 252, 313, and 697 nm with an intensity ratio of the bands at 252 and 313 nm (I_{252}/I_{313}) of 3.66. The principal band in the UV region is shifted by 10 nm relative to what we observe, and in our case the ratio of the bands at 245 and 315 nm (I_{245}/I_{315}) is >20. UV data for

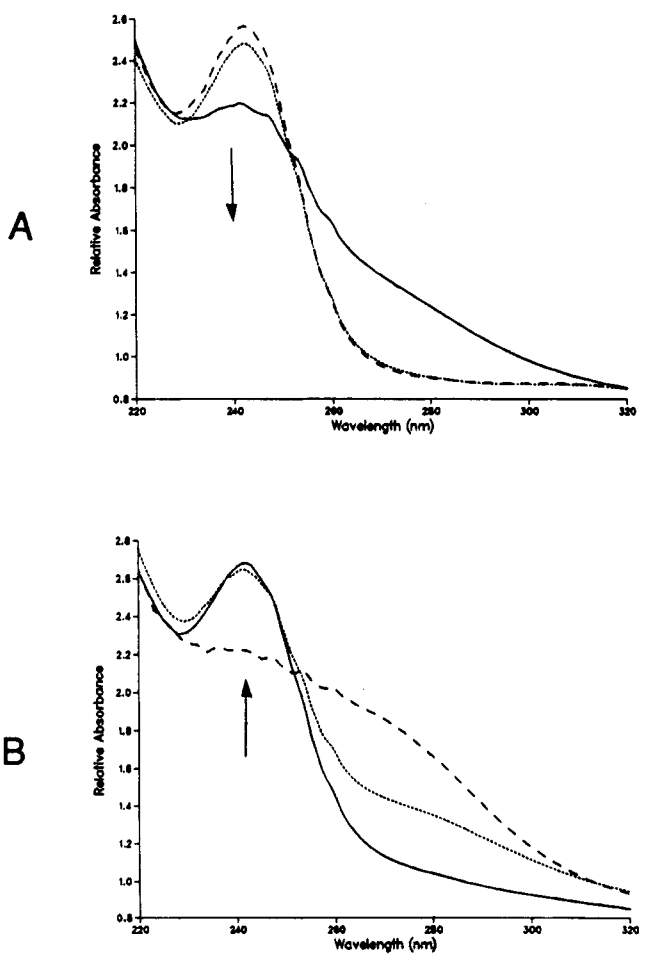

Figure 2. Spectral changes for the reduction of (Cp)Ti(C_7H_7) in THF/TBAP from 220 to 320 nm: (A) E = −2.20 V with (---) no applied potential, (···) t = 50 s, and (—) t = 120 s; (B) E = −0.20 V after application of the reducing potential with (---) E = −2.20 V, (···) t = 50 s, and (—) t = 120 s.

[(Cp)Ti(C_7H_7)]$^-$ were not reported, but the visible spectrum was characterized by a strong band at 579 nm, shifted by 29 nm from our reported spectra.[10] The band at 579 nm was assigned to the $^2A_1 \rightarrow {}^2E_1$ transition on the basis of MO calculations and data for (Cp)V(C_7H_7).

Table II. Spectroelectrochemical Data for (Cp)Ti(L) and (Cp*)Ti(L) in THF/TBAP

complex	applied potential,[a] V	λ_{max}, nm
(Cp)Ti(C_7H_7)	no potential[b]	242, 315, 700
	−2.20	252,[c] 280,[d] 510, 650[e]
(Cp*)Ti(C_7H_7)	no potential[b]	237[f]
	−2.50	237[c,f]
	1.00	237[c,f]
(Cp)Ti(C_8H_8)	no potential[b]	230, 711
	0.50	233, 500[d]
(Cp*)Ti(C_8H_8)	no potential[b]	241[f]
	0.20	245[f]

[a] Potential applied to working electrode vs a Pt-wire pseudo reference electrode. [b] Identical spectra were also obtained in a standard cell designed for inert atmosphere measurements in the absence of supporting electrolyte. [c] Peak does not shift, but there was a significant change in intensity (see text). [d] Broad increase in absorbance centered around this wavelength (see text). [e] Shoulder on a band. [f] Visible region not monitored.

The difference in the spectra for the reduced species presumably represents the difference between the chemical reduction product and $[(Cp)Ti(C_7H_7)]^-$. The reason for the difference in the reported spectral data and our data for (Cp)Ti(C_7H_7) is unknown.

Spectroelectrochemical data in the UV region for the reduction of (Cp*)Ti(C_7H_7) have the same general features as those found for (Cp)Ti(C_7H_7) and are summarized in Table II.

Oxidation of (Cp)Ti(C_7H_7) and (Cp*)Ti(C_7H_7). Figure 1B shows the cyclic voltammetric response for (Cp)Ti(C_7H_7) in THF/TBAP when the potential is scanned in a positive direction. One oxidation wave (wave 4, Figure 1B) at E_{pa} = 0.76 V vs SCE at 100 mV/s is found up to potentials of 1.50 V vs SCE. Wave 4 is characterized as a diffusion-controlled one-electron process, as evidenced by a constant value of $i_p/v^{1/2}$ and the fact that $E_{pa} - E_{pa/2}$ is 66 mV.[28] The value of E_{pa} shifts in a positive direction with an increase in the scan rate, and the electrochemical properties are consistent with an EC mechanism.[30]

A coupled re-reduction process is not found for wave 4 up to scan rates of 1000 mV/s. This suggests that a rapid chemical reaction follows the electron-transfer process and that the product is electrochemically inactive. Multiple scans in the cyclic voltammogram only indicate wave 4 and suggest that passivation of the electrode surface occurs after oxidation.

A one-electron-oxidation process is also found for compound 2 at E_{pa} = 0.50 V vs SCE in CH_2Cl_2/TBAP, but in CH_3CN/TBAP wave 4 is shifted to E_{pa} = 0.15 V vs SCE. Re-reduction waves coupled to wave 4 are again not found when either CH_2Cl_2 or CH_3CN is the solvent.

(Cp*)Ti(C_7H_7) in THF/TBAP is the same as that observed for (Cp)Ti(C_7H_7), with the exception that the potential is shifted due to the change of Cp* for Cp.[15] The data for (Cp*)Ti(C_7H_7) are summarized in Table I.

Figure 3A shows the spectral changes that occur upon oxidation of (Cp)Ti(C_7H_7) at 1.40 V in THF/TBAP. As shown in Figure 3A, the band at 242 nm initially decreases in intensity and slightly shifts to longer wavelengths. On longer time scales there is an increase in the absorbance, continued broadening of the band, and a shift back to 242 nm. In addition, there is a general increase in the absorbance over the spectral range from 320 to 360 nm. No isosbestic points are indicated in Figure 3A. Figure 3B demonstrates that no significant spectral changes occur when the potential is changed from +1.40 to −0.20 V. This is in agreement with the electrochemical data and suggests that an irreversible chemical reaction follows the oxidation

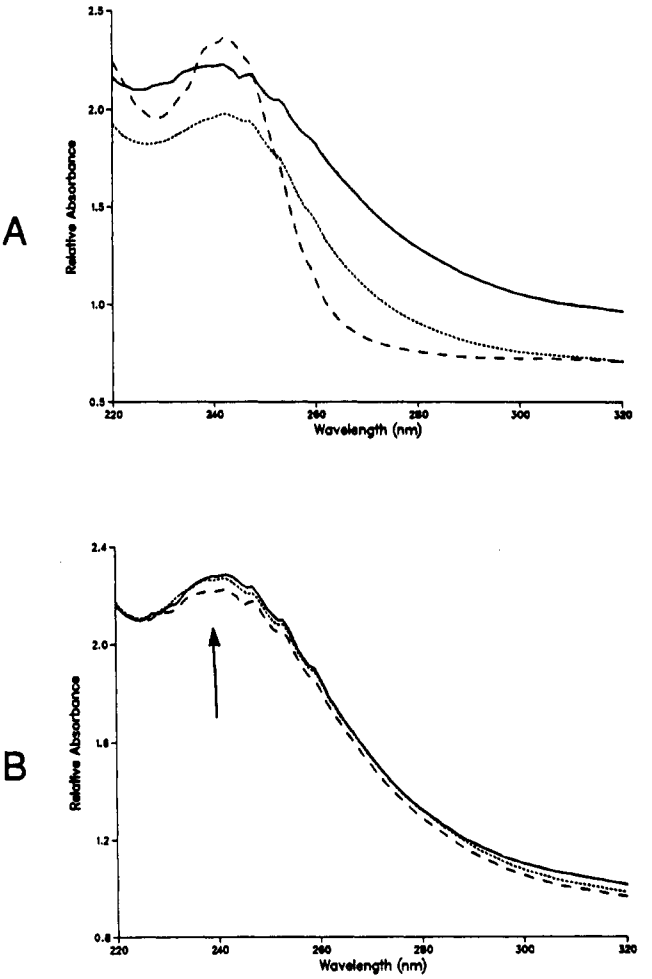

Figure 3. Spectral changes for the oxidation of (Cp)Ti(C_7H_7) in THF/TBAP from 220 to 320 nm: (A) E = 1.40 V with (---) no applied potential, (···) t = 50 s, and (—) t = 120 s; (B) E = −0.20 V after application of the oxidizing potential with (---) E = 1.40 V, (···) t = 50 s, and (—) t = 120 s.

Scheme I

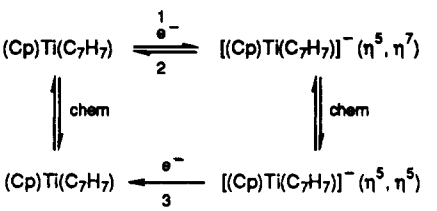

process. Spectral changes similar to those shown in Figure 3 are found for the oxidation of (Cp*)Ti(C_7H_7), and the data are summarized in Table II.

Electron-Transfer Mechanism of (Cp)Ti(C_7H_7) and (Cp*)Ti(C_7H_7). The reversible reduction product $[(Cp)Ti(C_7H_7)]^-$ has been previously characterized by ESR, ENDOR, and UV–visible spectroscopy.[10] On the basis of the results of these studies $[(Cp)Ti(C_7H_7)]^-$ was shown to have the same geometry as the parent species and the added electron was assigned to the a_1 orbital,[10] which is nearly all metal dz^2 character.[6] Our electrochemical data indicate that a box mechanism, as shown in Scheme I, describes the reductive electron-transfer properties for both (Cp)Ti(C_7H_7) and (Cp*)Ti(C_7H_7). Waves 1 and 2 (Figure 1A) correspond to the reversible reduction and re-oxidation of (Cp)Ti(C_7H_7), while wave 3 corresponds to the oxidation of the chemical reaction product. The observation of wave 2 depends upon the solution conditions, which implies that the chemical reaction rate following

reduction has a solvent dependence. A chemical reaction follows process 3 to regenerate (Cp)Ti(C_7H_7) and is relatively rapid since a reduction wave coupled to wave 3 is not observed.

The spectral data for reduction of complexes 2 and 4 give insight into the nature of the chemical reaction product. The decrease in the intensity of the band at 225 nm for complex 2 is not consistent with the simple addition of the electron to the a_1 orbital but suggests a strong perturbation of the ligand antiboding orbitals. The perturbation is most likely the result of a change in molecular geometry following electron transfer. The molecular change must be reversible and must be capable of occurring rapidly to be consistent with the cyclic voltammetric data. We favor a hapticity change in the C_7H_7 ring from η^7 to η^5 as the chemical reaction following reduction. Electrochemically induced hapticity changes in complexes of this type are well-documented.[13,18-20,22] The addition of a solvent molecule (or another ligand) following electron transfer is not likely, since this would result in the generation of a formal 19-electron species, assuming no other molecular changes.

Both (Cp)Ti(C_7H_7) and (Cp*)Ti(C_7H_7) undergo an irreversible chemical reaction following the abstraction of one electron, on the basis of the electrochemical results. The exact nature of the species generated in the chemical reaction after the oxidation is unkown. The spectroelectrochemical data in this case are not revealing and again probably reflect a change in the molecular structure via the following chemical reaction. The strong solvent dependence of E_{pa} is suggestive of reaction with the solvent after oxidation. Bulk electrolysis experiments result in abstraction of less than 0.2 electron per metal, consistent with multiple scan cyclic voltammetric experiments that indicated passivation of the electrode surface upon oxidation.

Electrochemistry of (Cp)Ti(C_8H_8) and (Cp*)Ti(C_8H_8). No reduction processes are found up to the solvent limit for complexes 1 and 3, and in both cases relatively easy oxidation processes are found. The oxidations of complexes 1 and 3 are shown in Figure 4, which demonstrates the cyclic voltammetric response for (Cp)Ti(C_8H_8) (Figure 4A) and (Cp*)Ti(C_8H_8) (Figure 4B) in THF/TBAP.

The oxidation of (Cp)Ti(C_8H_8) is characterized by a wave of E_{pa} = −0.30 V (wave 5, Figure 4A) and a wave at E_{pa} = −0.17 V (wave 6, Figure 4A) vs SCE on the first scan but only one oxidation wave on the second and all subsequent scans (wave 5). After the first scan through waves 5 and 6, only one reductive process is found at E_{pc} = −0.42 V vs SCE (wave 7, Figure 4A). Consistent with the shift found for the change in ligand,[15] E_{pa} values for wave 5 and 6 of (Cp*)Ti(C_8H_8) are −0.70 and −0.63 V, respectively, while E_{pc} for wave 7 is −0.77 V vs SCE at 60 mV/s as shown in Figure 4B. In all other aspects, the electrochemical behavior of (Cp*)Ti(C_8H_8) in THF/TBAP is identical with that found for (Cp)Ti(C_8H_8).

Wave 6 is a one-electron-oxidation wave evidenced by a $E_{pa} - E_{pa/2}$ value of 81 and 71 mV for complexes 1 and 3, respectively in Figure 4. On the first scan, wave 6 is the predominant oxidation process of complexes 1 and 3. The location of wave 6 is scan rate dependent, and the value of E_{pa} shifts to negative potentials as the scan rate is decreased. For example, wave 6 is at E_{pa} = −0.22 V vs SCE for complex 1 at 30 mV/s. It appears that i_5/i_6 increases as the scan rate is increased, but this is complicated by the fact that ΔE_p decreases as the scan rate is increased. At 1000 mV/s only one wave is observed.

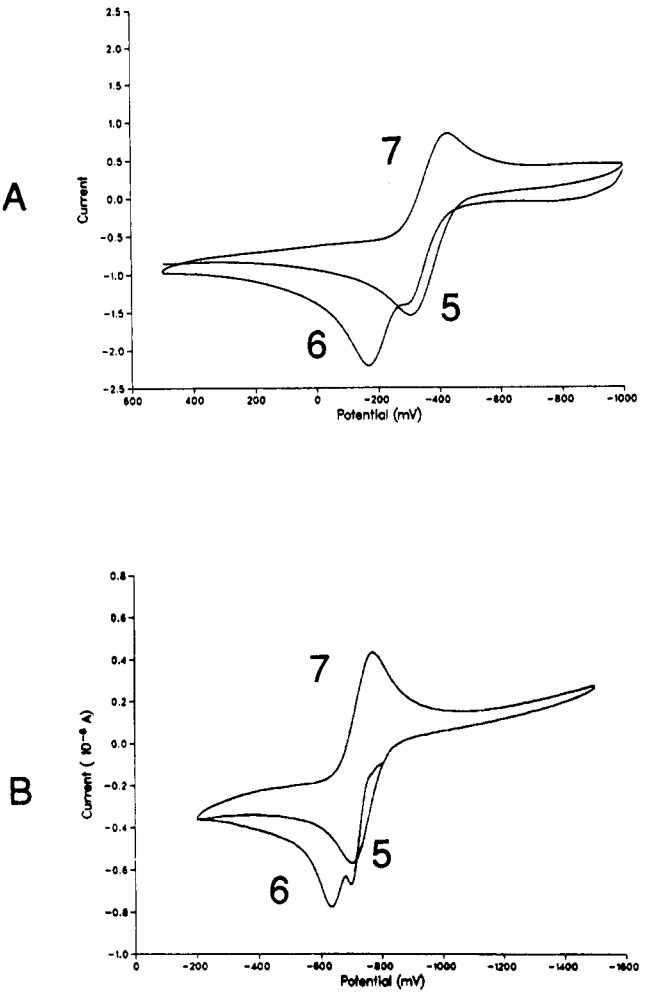

Figure 4. Cyclic voltammograms of (A) a solution of (Cp)Ti(C_8H_8) in THF/0.33 M TBAP, in a scan from −1.0 to +0.50 V vs SCE (scan rate 100 mV/s), and (B) a solution of (Cp*)Ti(C_8H_8) in THF/0.39 M TBAP, in a scan from −0.80 to −0.20 to −1.50 V vs SCE (scan rate 60 mV/s).

The dependence of waves 5 and 6 on the scan rate is rationalized by the presence of an equilibrium between two electroactive species, with the predominant solution species corresponding to wave 6. Under the influence of an applied potential the equilibrium between the species shifts and a change in i_5/i_6 occurs. There are several examples in the literature of how an applied potential can affect such an equilibrium process.[31-33] Bulk electrolysis at 0.50 V vs SCE gives 1.0 ± 0.1 electron per Ti for the oxidation of either (Cp)Ti(C_8H_8) or (Cp*)Ti(C_8H_8), which is in agreement with waves 5 and 6 corresponding to two forms of the same species.

Waves 5 and 7 correspond to a reversible one-electron-transfer process at $E_{1/2}$ = −0.36 V vs SCE for (Cp)Ti(C_8H_8) and at $E_{1/2}$ = −0.74 V vs SCE for (Cp*)Ti(C_8H_8). The value of $E_{pa} - E_{pc}$ is 116 mV in Figure 4A and is 68 mV in Figure 4B. For both complexes, the values of $E_{1/2}$, for waves 5 and 7, are constant with scan rate and the value of i_{pa} or $i_{pc}/v^{1/2}$ is constant on the second and all subsequent scans.

If the cyclic voltammetric scan is started positive of process 6, only waves 5 and 7 are observed for (Cp)Ti(C_8H_8) or (Cp*)Ti(C_8H_8). However, under these conditions

(31) Kadish, K. M.; Bottomley, L. A. *Inorg. Chem.* **1983**, *22*, 342.
(32) Kadish, K. M. *Prog. Inorg. Chem.* **1986**, *34*, 435.
(33) Kadish, K. M.; Bottomley, L. A. *J. Chem. Soc., Chem. Commun.* **1981**, 1212.

an oxidative current is found at the start of the scan and the cyclic voltammogram is for the electrogenerated monoanion.

The electrochemical behavior of $(Cp)Ti(C_8H_8)$ and $(Cp^*)Ti(C_8H_8)$ is dependent upon the solvent conditions, which are summarized in Table I. The most significant change is observed for $(Cp)Ti(C_8H_8)$ in CH_3CN/TBAP, in which wave 6 is not observed. In addition, if CH_2Cl_2/TBAP is used with either $(Cp)Ti(C_8H_8)$ or $(Cp^*)Ti(C_8H_8)$, a chemical oxidation occurs, and only waves 5 and 7 are found. The chemical reaction with CH_2Cl_2 will be discussed later in the text.

If $TBA(BF_4)$ rather than TBAP is used as the supporting electrolyte, with THF, a reversible electron transfer is found at $E_{1/2}$ = −0.55 and −0.72 V vs SCE for $(Cp)Ti(C_8H_8)$ and $(Cp^*)Ti(C_8H_8)$, respectively. If this potential is standardized, via ferrocene, to the data obtained with TBAP, the reversible couple corresponds to wave 6. This implies that wave 6 can also be reversible under the proper solution conditions.

Electrochemical data for $(Cp)Ti(C_8H_8)$ have been reported,[23] and a reversible one-electron oxidation at $E_{1/2}$ = −0.50 vs SCE was found in THF/$TBA(PF_6)$. Only a reversible electron-transfer process was observed, in agreement with our measurements performed in the absence of perchlorate anion, but the value for $E_{1/2}$ is shifted from our data.

For $(Cp^*)Ti(C_8H_8)$, bulk electrolysis was performed on a preparative scale to allow characterization of the one-electron-oxidation product. Under these conditions, an orange precipitate formed as the oxidation progressed. The precipitate was collected, washed twice with THF to eliminate any excess TBAP, and vacuum-dried for approximately 12 h. The cyclic voltammogram obtained for this species in THF/TBAP only exhibited waves 5 and 7, which is in agreement with that found in the electrochemical analysis of $(Cp^*)Ti(C_8H_8)$.

A singlet at 7.12 ppm and a singlet at 1.79 ppm, with an integration ratio of 8:15, are observed in the ^1H NMR spectrum for the oxidized species in CD_3CN. The peak at 1.79 ppm is due to the Cp* ring, while the peak at 7.12 ppm is due to the cyclooctatetraene ring,[2] and since both peaks are singlets, the protons are equivalent for their respective rings on the NMR time scale. No other peaks are found in the NMR spectrum, and hence, the oxidation does not result in degradation of either ring. In agreement, chemical oxidation of $(Cp)Ti(C_8H_8)$ with iodine is reported to form $(Cp)Ti(C_8H_8)I$.[34] The electronic spectrum of the oxidation product is characterized by a strong absorption band at 245 nm. IR spectra indicated the presence of perchlorate ion in the oxidized species.

The addition of $(Cp^*)Ti(C_8H_8)$ to methylene chloride results in the chemical oxidation of this species. This is evidenced by a change in solution color from green to orange and the formation of a orange precipitate. By both cyclic voltammetric and UV–visible analysis, this species is the same as the product obtained by bulk electrolysis.

Figure 5A shows the spectroelectrochemical results between 320 and 220 nm obtained for the oxidation of $(Cp)Ti(C_8H_8)$ at 0.50 V vs SCE in THF/TBAP. In this spectral region, $(Cp)Ti(C_8H_8)$ has an absorption band at 230 nm, which upon oxidation slightly increases in intensity and shifts to 233 nm. When the potential is applied to −1.0 V vs SCE, the original spectrum is regenerated as shown in Figure 5B, which implies reversibility on the spectroelectrochemical time scale. In the visible region,

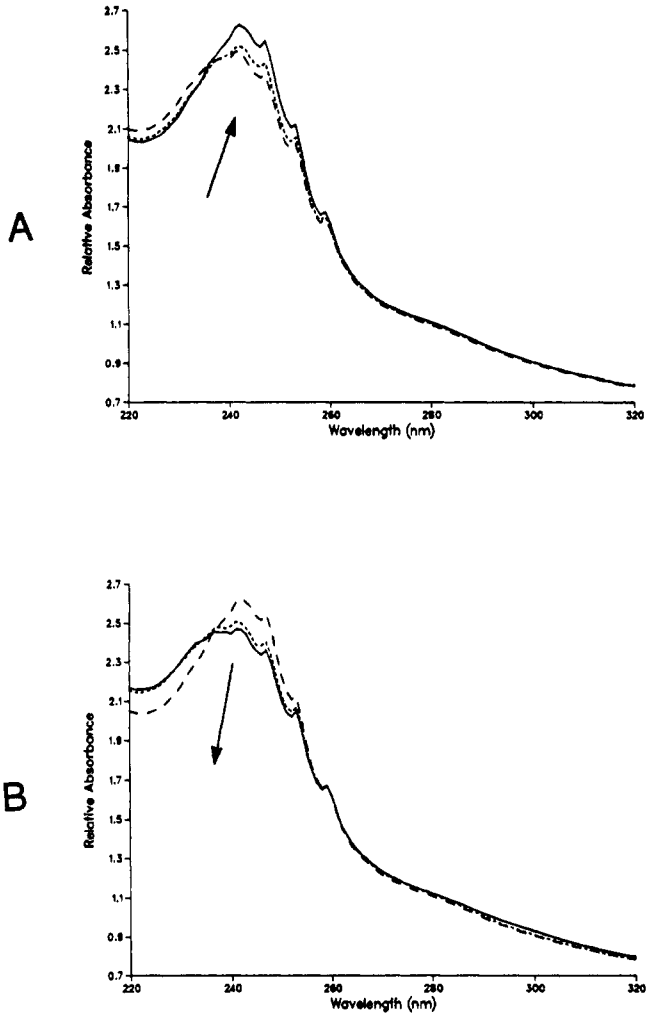

Figure 5. Spectral changes for the oxidation of $(Cp)Ti(C_8H_8)$ in THF/TBAP from 220 to 320 nm: (A) E = 0.50 V with (---) no applied potential, (···) t = 50 s, and (—) t = 120 s; (B) E = −1.0 V after application of the oxidizing potential with (---) E = 0.50 V, (···) t = 50 s, and (—) t = 120 s.

Scheme II

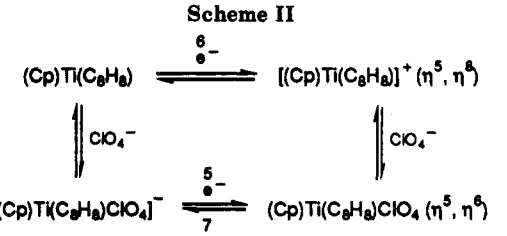

oxidation of $(Cp)Ti(C_8H_8)$ results in a decrease of the absorption band at 711 nm and the appearance of a band at 500 nm with an isosbestic point at 585 nm. Re-reduction results in generation of the original spectrum.

Spectroelectrochemical data for $(Cp^*)Ti(C_8H_8)$ in THF/TBAP are similar to those obtained for $(Cp)Ti(C_8H_8)$. The neutral complex is characterized by a strong band at 240 nm in the UV region, which upon oxidation shifts to 245 nm. The final spectrum is identical with that found for the oxidation product obtained by bulk electrolysis. Re-reduction of the oxidized species results in the observation of the original solution spectrum. Table II provides a summary of the spectroelectrochemical data for these species.

Electron-Transfer Mechanism of $(Cp)Ti(C_8H_8)$ and $(Cp^*)Ti(C_8H_8)$. The electrochemical and spectroelectrochemical data for these two compounds are consistent with

(34) Van Owen, H. O.; Meijer, H. J. L. *J. Organomet. Chem.* **1975**, *8*, 227.

the electron-transfer mechanism presented in Scheme II for $(Cp)Ti(C_8H_8)$. In the presence of TBAP, two species are present in solution, $(Cp)Ti(C_8H_8)$ and the perchlorate adduct $[(Cp)Ti(C_8H_8)ClO_4]^-$. Waves 5 and 7 are assigned to the reversible electron transfer of the perchlorate adduct, while wave 6 is assigned to the oxidation of $(Cp)Ti(C_8H_8)$. The electrochemical properties of waves 5 and 6 suggest that observation of the perchlorate adduct on the first scan (wave 5) is due to the application of the potential and does not reflect bulk solution concentrations. In the absence of perchlorate anion, the reversible oxidation of either $(Cp)Ti(C_8H_8)$ or $(Cp^*)Ti(C_8H_8)$ is found.

It is interesting that $(Cp)Ti(C_8H_8)$ in CH_3CN/TBAP does not show the presence of two species. This could be due to a significant change in the chemical reaction kinetics, but we think it is evidence of coordination of $(Cp)Ti(C_8H_8)$ by acetonitrile.

The oxidation product in the presence of perchlorate is assigned as $(\eta^5\text{-}Cp)Ti(\eta^6\text{-}C_8H_8)(ClO_4)$, since the second and all subsequent scans in the cyclic voltammogram show only waves 5 and 7. The agreement between the electronic spectra of the bulk electrolysis product and the spectroelectrochemical data suggest that this species is relatively stable. The equivalence of the protons on the NMR time scale neither supports nor negates this assignment.[2,3,8,9]

The results from MO calculations[4,5] and ESR,[8] ENDOR,[9] and photoelectron studies[11] all indicate the location of the unpaired electron in the C_8H_8 adducts is the a_1 orbital, which is primarily metal dz^2 character. The spectroelectrochemical data are consistent with these results in that the spectral changes indicate only a small perturbation of the ligand $\pi \rightarrow \pi^*$ absorption band.

Discussion

The spectroelectrochemical data provide information on the nature of the electrogenerated species, including insight into the electronic structure. However, the data for this set of complexes and for $(Cp)_2Ti(bpy)$[14] suggest that *assignment* of the site of electron transfer by spectroelectrochemical methods for organometallic species is not reliable. This is the case for (at least) two reasons. The first is that the chemical reactions that follow electron transfer typically result in significant changes in the electronic absorption spectra of the complexes and a separation of the effects due to the electron transfer and the chemical reaction is then required. The second reason is that the HOMO and LUMO cannot reliably be described as either ligand or metal centered. For example, the HOMO of $(Cp)Ti(C_7H_7)$ contains approximately 60% C_7H_7 character and 40% metal character,[6] while the HOMO of $(Cp)Ti(C_8H_8)$ is nearly 100% metal character.[4,5]

The large effect of the change from L = C_7H_7 to L = C_8H_8 on the electrochemical results is consistent with the electron-donating abilities of the respective ligands. The formal charge on the C_8H_8 ring is −2 and is +1 for C_7H_7. Hence, the observation of reduction processes for the 16-electron $(Cp)Ti(C_7H_7)$ or $(Cp^*)Ti(C_7H_7)$ species reflects the decrease in electron density on the complexes. The easy oxidation of the 17-electron $(Cp)Ti(C_8H_8)$ or $(Cp^*)Ti(C_8H_8)$ and the lack of observation of a reduction process is also consistent. However, it should be pointed out that MO calculations for both of these species result in a charge on the rings that is significantly different from the formal charge.[4-6] The difference between the oxidation potentials for the cyclooctatetraene adducts and the tropylium ion adducts is approximately 1 V. If one assumes that the energy difference between the HOMO and the LUMO is approximately the same for these species, then one would predict a reduction potential for the cyclooctatetraene adducts to be near 3.0 V vs SCE.

Acknowledgment is made by J.E.A. to the donors of the Petroleum Research Fund, administered by the American Chemical Society, for the support of this research.

Registry No. $(Cp)Ti(C_7H_7)$, 51203-49-7; $(Cp)Ti(C_7H_7)^-$, 115338-78-8; $(Cp)Ti(C_7H_7)^+$, 132854-60-5; $(Cp^*)Ti(C_7H_7)$, 104453-33-0; $[(Cp^*)Ti(C_7H_7)]^-$, 132774-48-2; $[(Cp^*)Ti(C_7H_7)]^+$, 132774-49-3; $(Cp)Ti(C_8H_8)$, 11065-40-0; $[(Cp)Ti(C_8H_8)]$, 57208-15-8; $(Cp^*)Ti(C_8H_8)$, 104469-59-2; $[(Cp^*)Ti(C_8H_8)]^+$, 132774-50-6; $[(Cp^*)Ti(C_8H_8)]ClO_4$, 132774-51-7; TBAP, 1923-70-2; $TBA(BF_4)$, 429-42-5; THF, 109-99-9; CH_3CN, 75-05-8; CH_2Cl_2, 75-09-2.

Molecular Self-Recognition and Crystal Building in Transition-Metal Carbonyl Clusters: The Cases of $Ru_3(CO)_{12}$ and $Fe_3(CO)_{12}$

Dario Braga* and Fabrizia Grepioni

Dipartimento di Chimica "G. Ciamician", Università di Bologna, Via Selmi 2, 40126 Bologna, Italy

Received June 22, 1990

The construction of the organometallic crystals of $Ru_3(CO)_{12}$ and $Fe_3(CO)_{12}$ has been investigated by means of potential energy calculations and computer graphic analysis. It has been found that the crystallization process is based on the recognition of some simple packing motifs over the molecular surface that depend on the shape of the carbonyl coverage. The crystals of $Ru_3(CO)_{12}$ and $Fe_3(CO)_{12}$ are constructed via the interlocking of tetra-, tri-, and dicarbonyl units of independent molecules. New insights in the disorder of $Fe_3(CO)_{12}$ have been gained.

Introduction

The fundamental contribution made by X-ray crystallography to the understanding of chemical properties of organometallic compounds is evidenced by the large number of crystal structures reported to date. It has been less appreciated, however, that these diffraction studies also provide basic information about the molecular organization within the crystal lattice, on the intermolecular forces, and on the influence that these intermolecular forces have on the structural features. It would appear that most chemists (and crystallographers) are accustomed to regarding a *molecular* structure as the ultimate result of a *crystal*

0276-7333/91/2310-1254$02.50/0